Evolution of the magnetic ground state in the electron-doped antiferromagnet CaMnO$_3$

A. L. Cornelius and B. E. Light

Department of Physics, University of Nevada, Las Vegas, Nevada 89154-4002, USA

J. J. Neumeier

Department of Physics, Montana State University, Bozeman, Montana 59717, USA

Measurements of the specific heat on the system Ca$_x$MnO$_3$ ($x \leq 0.10$) are reported. Particular attention is paid to the effect that doping the parent compound with electrons by substitution of La for Ca has on the magnetic ground state. The high- ($T > 40$ K) temperature data reveal that doping decreases T_N from 122 K for the undoped sample to 103 K for $x = 0.10$. The low temperature ($T < 20$ K) heat-capacity data are consistent with phase separation. The undoped sample displays a finite density of states and typical antiferromagnetic behavior. The addition of electrons in the $x \leq 0.03$ samples creates local ferromagnetism as evidenced by a decreased internal field and the need to add a ferromagnetic component to the heat-capacity data for $x = 0.03$. Further substitution enhances the ferromagnetism as evidenced by the formation of a long-range ferromagnetic component to the undoped antiferromagnetic structure. The results are consistent with a scenario involving the formation of isolated ferromagnetic droplets for small x that start to overlap for $x \approx 0.06$ giving rise to long range ferromagnetism coexisting with antiferromagnetism.

I. INTRODUCTION

Electronic phase segregation in transition-metal oxide systems has become an important topic in condensed-matter physics.[1–5] Systems which exhibit colossal magnetoresistance (CMR), high-temperature superconductivity, and other compounds such as the nickelates,[6] phase segregate into electron-rich and electron-poor regions. These phase segregated regions are known to order and form a stripe phase,[5] or the atomic orbitals of the transition-metal ions themselves[7] sometimes order. Theoretical descriptions of the large magnetoresistance observed in CMR oxides is currently focused on numerous approaches, but the phase-segregation scenario, where charge inhomogeneous regions compete with ferromagnetism,[1–3] is currently receiving a great deal of attention. In this picture, the application of magnetic field, or decreasing the temperature, alters the ratio of these phase segregated regions thereby affecting the electrical conductivity. In the case of high-temperature superconductors, the possible relation between the stripe phase and superconductivity is under debate, but some believe that the stripes are crucial to the formation of a superconducting ground state in the cuprates.[8,9]

Some recent studies on Ca$_{1-x}R_x$MnO$_3$ revealed that doping with a trivalent ion R^{3+} (R = La, Pr, Sm, Gd, Eu, Ho, or Bi) leads to the formation of a small ferromagnetic (FM) moment.[10–13] This effect was subsequently investigated in greater detail[14] where the FM moment at 5 K M_{sat}(5 K) was found to display two distinct regimes for La dopings $x < 0.08$. In the range $0 \leq x \leq 0.02$, the doped electrons appear to remain essentially localized on Mn sites leading to isolated Mn^{3+} ions which coexist with the majority Mn^{4+} ions. This leads to a ferromagnetic moment, shown through a phenomenological model, consistent with the existence of local ferrimagnetism. That is, each doped electron creates one local ferrimagnetic site. Doping in the range $0.03 \leq x \leq 0.07$

leads to improved electrical conductivity and a FM moment which has a stronger x dependence. The observed moment is consistent with the existence of local ferromagnetic regions. This picture of local ferromagnetic regions coexisting within an antiferromagnetic (AFM) background is supported by recent NMR experiments,[15] theoretical treatments,[16] and neutron powder-diffraction experiments.[17,18] Neutron powder diffraction has revealed that the region $0 \leq x \leq 0.07$ indeed contains a mixture of G-type antiferromagnetism and ferromagnetism which for $x = 0.06$ appears to have a long-range component. A sample of $x = 0.02$ reveals, through small-angle neutron scattering (SANS), ferromagnetic clusters of diameter 10 Å; these clusters overlap at larger x values leading to long-range ferromagnetism at $x = 0.06$.[17] Concentrations of $x > 0.7$ lead to formation of the C-type antiferromagnetic phase which coexists over a wide temperature and concentration range with the G-type phase ($0.07 \leq x < 0.2$).[18] These results suggest that the Ca$_{1-x}R_x$MnO$_3$ system is ideal for the study of electronic/magnetic phase segregation in the low doping limit where FM phase segregated regions begin their nucleation within an AFM host. The present work involves heat capacity studies of some of these systems.

II. EXPERIMENTAL DETAILS

The specimens were synthesized under identical conditions to minimize variations attributable to chemical defects.[19] Stoichiometric quantities of (99.99% purity or better) CaCO$_3$, La$_2$O$_3$, and MnO$_2$ were weighed and mixed in an agate mortar for 7 min followed by reaction for 20 h at 1100 °C. The specimens were reground for 5 min, reacted for 20 h at 1150 °C, reground for 5 min, reacted for 20 h at 1250 °C, reground for 5 min, reacted for 46 h at 1300 °C, reground for 5 min, pressed into pellets, reacted for 17 h at 1300 °C, and cooled at 0.4 °C/min to 30 °C. Powder x-ray diffraction revealed no secondary phases and iodometric ti-
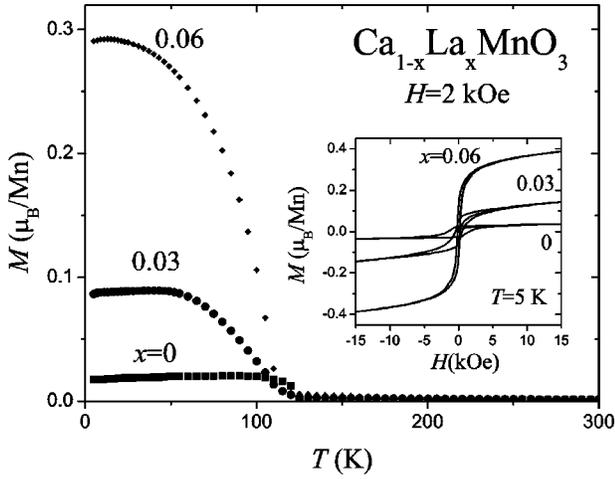
FIG. 1. Magnetization M versus temperature in an applied field of 2 kOe for $Ca_{1-x}La_xMnO_3$ specimens. In the inset M versus magnetic field H at 5 K is displayed.

tration, to measure the average Mn valence, indicates the oxygen content of all specimens falls within the range 3.00 ± 0.01. Magnetic measurements were conducted with a superconducting quantum interference device magnetometer. Heat-capacity measurements, using a standard thermal relaxation method, were performed on a Quantum Design PPMS system equipped with a superconducting magnet capable of generating a 90-kOe magnetic field.

III. RESULTS AND DISCUSSION

A. Magnetization

Magnetization as a function of temperature $M(T)$ at 2 kOe is displayed for three of the $Ca_{1-x}La_xMnO_3$ specimens of this study in Fig. 1. The $x=0$ sample, $CaMnO_3$, exhibits an antiferromagnetic transition at $T_N=131$ K. A weak ferromagnetic component is evident in the data, which is generally attributed to canting of the AFM moments, although recent work[14] suggests that it arises from a small defect concentration. Substitution of La for Ca enhances the saturation moment in a systematic fashion as described previously.[14] M versus magnetic field H data at 5 K are displayed in the inset of Fig. 1, illustrating a typical ferromagnetic response. The saturation moment at 5 K can be extracted from the data in the inset by drawing straight lines through the two linear portions of the curves; the intersection point of these lines is defined as $M_{sat}(5 \text{ K})$.[14] As mentioned above, M_{sat} was shown to possess a systematic dependence on x consistent with the formation of isolated FM regions for small dopings that cross over to AFM order with a long-range FM component. This behavior in Ref. 14 revealed that beyond $x=0.08$ AFM C-type regions began to nucleate, which is consistent with simple statistical arguments.[20] These results are consistent with the scenario of small ferromagnetic clusters appearing at low concentrations ($0<x\leq0.3$) that begin to overlap into long-range ferromagnetism at higher doping ($x\approx0.06$) and to a coexistence of G- and C-type AFM with a long-range FM component for $x>0.08$.

B. Low-temperature specific heat

The low-temperature specific-heat measurements were performed over the temperature range with no applied magnetic field. The total specific heat can be written as

$$C_p = C_{elec} + C_{mag} + C_{hyp} + C_{lat}, \tag{1}$$

where C_{elec} is the electronic contribution, C_{mag} is from the Mn magnetic moments, C_{hyp} is from the nuclear moment of ^{55}Mn, and C_{lat} is due to the lattice. The electronic contribution is given by γT, where γ is the Sommerfield coefficient which is related to the density of electronic states at the Fermi energy. C_{hyp} is given by A/T^2 where A is related to the internal hyperfine magnetic field by the relation[21]

$$A = \frac{R}{3}\left(\frac{I+1}{I}\right)\left(\frac{\mu H_{hyp}}{k_B}\right)^2, \tag{2}$$

where I is the nuclear moment (5/2 for ^{55}Mn), μ is the nuclear magnetic moment (3.45 nuclear magnetons for Mn), and H_{hyp} is the internal field strength at the Mn site. C_{lat} is estimated by the approximation $C_{lat}=\beta_{3l}T^3$. The Debye temperature Θ_D is given by

$$\Theta_D = \left(\frac{1.944\times10^6 \ r}{\beta_{3l}}\right)^{1/3}, \tag{3}$$

where β_{3l} is in mJ/mol K^4 and r is the number of atoms per unit cell. Due to the small variation in chemical composition in the measured samples, it was assumed that β_{3l}, and therefore Θ_D, are the same for all three samples (this assumption seems valid when looking at the results of Lees et al. who found a variation in Θ_D of less than 1.5% over a much larger range of substitutions[21] and our own finding that Θ_D from our high-temperature data is 650 ± 10 for all five samples). Like other reports,[21,22] we added a T^5 term to adequately fit the lattice heat-capacity data. C_{mag} is estimated as $\Sigma \beta_n T^n$ where the value of the exponent n corresponds to the type of magnetic excitation ($n=3$ for AFM, $n=3/2$ for FM, $n=2$ for a possible long-wavelength spin excitation[22]). For AFM and FM excitations with a nonzero gap, the heat-capacity coefficients are related to the spin-wave stiffness D by the relation $\beta_n=ck_B(k_BT/D)^n$ where c is a constant that depends on the lattice type.[21] One plausible scenario leading to a T^2 term is the existence of a long-wavelength spin-wave excitation with a planar FM component of stiffness D_ρ and a linear component D_z with $\beta_n\propto(D_\rho D_z)^{-1}$.[22]

The low-temperature measurements are shown in Fig. 2. For $x=0$, the data can be fit well using Eq. (1) as seen by the solid line. Since the sample is known to have G-type AFM order (each Mn magnetic moment is aligned antiparallel to its neighbor),[23] it is expected that $\beta_{mag}=\beta_{3m}T^3$. Since the lattice term is also proportional to T^3, the total T^3 term β_3 will be $\beta_{3l}+\beta_{3m}$, and it is impossible to separate the magnetic and lattice components, without prior knowledge of the Θ_D, from the low-temperature data. However, since the high-temperature values of Θ_D are all similar, any variation we find in β_3 should be mostly due to β_{3m}. The parameters which give the best fits to the data are shown in Table I. From the fit parameters, we can arrive at the following con-
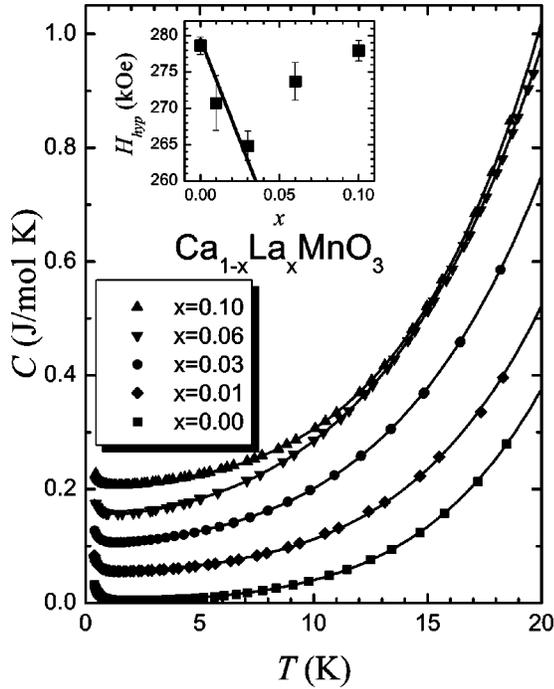
FIG. 2. Measured specific heat as a function of temperature for $Ca_{1-x}La_xMnO_3$. The lines are fits described in text with the relevant fitting parameters summarized in Table I. Subsequent curves were offset for clarity. The inset shows the internal magnetic field H_{hyp} at the Mn site as deduced from the nuclear contribution to the heat capacity.

clusions. The value of β_5 does not vary much from sample to sample, which gives us confidence that our fitting parameters are not skewed by the addition of this term. There exists a nonzero electronic term γ indicative of a finite value of the density of states at the Fermi level, consistent with thermopower measurements.[12] Since the data can be fit to a form $\beta_n T^n$ leads to the conclusion that there is not a gap in the spin-wave excitation which often requires an activated term to describe the heat capacity. The hyperfine term for the undoped sample corresponds to an internal field of 279 kOe, which is ~30% less than found for $LaMnO_3$,[22] but a factor of 2.6 smaller than determined for $Pr_{0.6}Ca_{0.4}MnO_3$.[21]

The lines in Fig. 1 are fits to the data using Eq. (1) with the values for n which give the best fits to the data. The fit

TABLE I. Summary of the fitting parameters to the data in Fig. 2. Definitions of the various coefficients are given in the text. The units are kOe for H_{hyp}, mJ/mol K^2 for γ, and mJ/mol K^{n-1} where n is the subscript of the coefficient. The number in parentheses is the statistical uncertainty in the last digit from the least-squares-fitting procedure.

x	H_{hyp}	γ	$10^3\beta_3$	$10^5\beta_5$	$\beta_{3/2}$	β_2
0	279(1)	1.38(3)	2.09(2)	5.64(4)		
0.01	271(3)	2.44(5)	3.26(5)	5.06(9)		
0.03	265(2)	1.46(9)	4.47(7)	4.94(9)	1.17(6)	
0.06	274(2)	1.98(8)	3.29(2)	6.95(9)		0.76(2)
0.10	279(2)	2.76(9)	5.89(6)	8.17(7)	0.35(2)	

parameters are summarized in Table I. The introduction of the electron dopants leads to an increase in γ as one would expect. For $x=0.01$ adding an $n=3/2$ or $n=2$ component does not significantly improve the fit. Rather only an increase in the AF term β_3 (note that a larger value of β_3 relative to the undoped sample corresponds to a smaller spin-wave stiffness) and a decrease H_{hyp} are found. For $x=0.03$, we find that there is a need to add a FM ($n=3/2$) term in addition to a larger AFM ($n=3$) term relative to the $x=0$ value to fit the data. The value of $H_{hyp}=265$ kOe is reduced relative to the undoped sample. One scenario that would lead to a reduced internal magnetic field would be for the doped electrons to reside on a Mn site with a spin antiparallel to the original spin, and larger in magnitude. This would change the local environment around the doped Mn ion to FM while reducing the average AFM magnetic moment (and thus H_{hyp}) and would lead to a local distortion or FM polaron. This scenario would lead to a linear decrease in H_{hyp} as x increases. This is exactly what is observed for small values of x in the inset to Fig. 2, where the line represents H_{hyp} decreasing 1.6% per percent of La substitution. The fact that H_{hyp} changes faster than x is consistent with the moments antiparallel to the original spin moments being larger in magnitude.

These results are in agreement with magnetization measurements which were also interpreted in terms of the formation of local FM regions (FM polarons)[14] and SANS measurements that show small ferromagnetic droplets.[17] In this scenario, one would envision the weakening of the AFM spin-density wave and the formation of FM excitations; which is exactly the result of the current measurements. These results agree with the strong weakening in the AFM interaction recently deduced from Raman scattering and electron paramagnetic resonance studies.[24]

As doping is increased above 0.03 we see a definite crossover in all of the heat-capacity data. For $x=0.06$, the data can no longer be fit by a simple FM term, and in fact the $n=3/2$ component is no longer observed (fitting with a 3/2 term yields a negative value for γ). Now an AFM ($n=3$) term plus a spin-density wave ($n=2$) term are needed. The magnitude of the AFM term decreases and the hyperfine term increases and is nearly the same as the undoped value. This leads to the conclusion that the nature of the magnetic excitations has changed and that there might no longer be local FM polarons. As mentioned, the T^2 term can be indicative of a long-wavelength excitation with both FM and AFM components. These results are in excellent agreement with the finding of isolated ferromagnetic droplets in an $x=0.02$ sample which merge into a long range ferromagnetic component for $x=0.06$.[17] This is consistent with a recent calculation[16] predicting a phase transition from the FM polaron state to a long-range FM state at a doping of $x\simeq0.045$ and experimental findings that there is a crossover from the magnetoelastic polaron to spin-canted phase around $x=0.06$.[25] Even higher concentrations ($x=0.10$) are again best fit with a FM $n=3/2$ term and a larger $n=3$ term. This is consistent with neutron-scattering results that
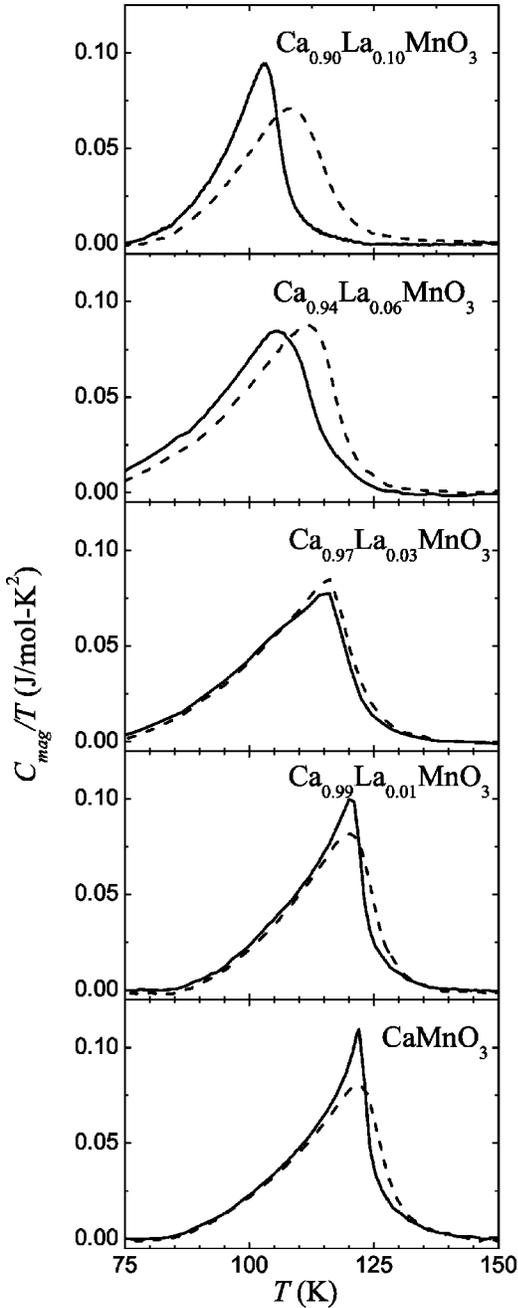
FIG. 3. Measured magnetic heat capacity C_{mag} as a function of temperature T in zero applied field (solid lines) and a 90-kOe magnetic field (dashed lines).

show the coexistence of C- and G-type AF order at this concentration[18] and magnetization measurements that show a ferromagnetic moment.

C. High-temperature specific heat

For the high-temperature data, C_{mag} is the contribution associated with the magnetic ordering transitions around T_N. The high-temperature measurements of C_{mag}/T are shown in Fig. 3. In this temperature range C_{hyp} is negligible. The background lattice contribution was estimated by fitting the measured Debye temperatures above and below the magnetic
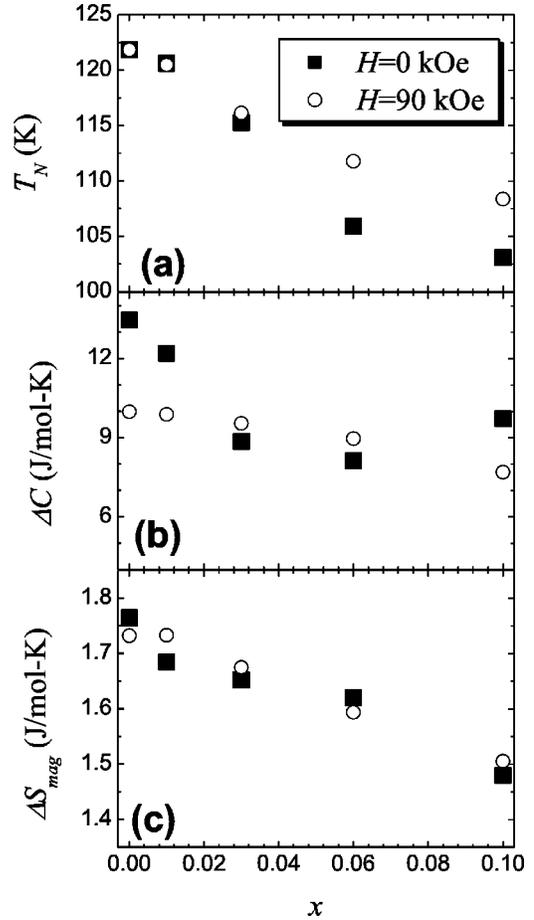

FIG. 4. Parameters obtained from the data shown in Fig. 3. Solid squares correspond to the zero-field data, while open circles correspond to data taken in a 90-kOe applied magnetic field. (a) The magnetic ordering temperature. (b) The peak value of the magnetic heat capacity ΔC_{mag}. (c) Change in magnetic entropy ΔS_{mag}, found by integrating C_{mag}/T as a function of T.

transitions with a polynomial. After subtracting this contribution, we are left with C_{mag}. For $CaMnO_3$ a magnetic transition is seen at $T_N = 122$ independent of the applied magnetic field. Doping electrons lowers T_N as seen in Fig. 4(a). In zero field, the decrease in T_N is linear followed by a more rapid drop for $x > 0.3$. In a 90-kOe field, the magnetic ordering temperature obeys a nearly linear relationship with x. In a similar manner to $CaMnO_3$, the $x = 0.01$ and 0.03 samples do not show a variation in T_N as the magnetic field is increased. This is to be expected as $k_B T_N \gg \mu_B H$ and the applied field should not alter the antiferromagnetic ordering temperature. This is not the case for the $x = 0.06$ and $x = 0.10$ samples where T_N steadily increase in applied field. This increase could be related to an enhancement of the FM neutron diffraction peak intensity observed in recent experiments,[18] where at $x = 0.12$ FM peak intensity was seen to increase at the expense of G-type AFM peak intensity in applied magnetic field. In other words, a long-range ferromagnetic component to the magnetic structure appears to be present for $x = 0.06$ and $x = 0.10$ due to the large enhancement of the magnetic ordering temperature in an applied

field. The jump in the magnetic heat capacity ΔC_{mag} at T_N is shown in Fig. 4(b). The value for the undoped sample is in good agreement with the work of Moritomo $et\ al.$[26] As x increases, ΔC_{mag} decreases, in sharp contrast to Moritomo $et\ al.$[26] In a 90-kOe field, the value of ΔC_{mag} is nearly independent of x. To obtain the change in entropy associated with the magnetic transition ΔS_{mag} we have integrated C_{mag}/T versus T and the results are shown in Fig. 4(c). Since it is difficult to accurately estimate the lattice contribution to the heat capacity, the absolute values of ΔS_{mag} have a reasonable amount of uncertainty. However, changes in ΔS_{mag} should be much more reliable since the lattice contribution was estimated in a systematic manner. For all values of x there appears to be little field dependence to ΔS_{mag}. For $x = 0$ an entropy of ~ 1.77 which corresponds to is found. This value is much smaller than the value one would expect from Ising spins ($R \ln 2$) or spin-3/2 Heisenberg spins ($R \ln 4$) perhaps due to domain formation. The magnetic entropy appears to decrease in a nearly linear fashion in a manner similar to the magnetic ordering temperature.

IV. CONCLUSION

We have performed measurements of the specific heat on the system $Ca_{1-x}La_xMnO_3$ ($x \leq 0.10$) to complement previous magnetization results. The high- ($T > 40$ K) temperature data show that doping decreases the value of T_N from 122 K for the undoped sample to 103 K for $x = 0.10$. The low-temperature ($T < 20$ K) heat-capacity data are consistent with phase separation. The undoped ($x = 0$) sample displays AFM order and has a finite density of states. When a small amount of holes ($x \leq 0.03$) are doped into the sample, local ferromagnetism is introduced into the system. Further substitution to $x = 0.06$ leads to long-range ferromagnetism as evidenced by the formation of a long-range spin-density wave. These results clearly show the utility of a thermodynamic measurement (heat capacity) in understanding the evolution of magnetic properties in electron doped $CaMnO_3$; namely for small dopings small ferromagnetic droplets form which upon further doping overlap and lead to long-range ferromagnetic order coexisting with antiferromagnetic order.

[1] E. Dagotto, T. Hotta, and A. Moreo, Phys. Rep. **344** , 1 (2001).

[2] A. Moreo, S. Yunoki, and D. Dagotto, Science **283**, 2034 (1999).

[3] C. N. R. Rao and A. K. Cheetham, Science **276**, 911 (1997).

[4] B. G. Levi, Phys. Today **51** (6), 19 (1998).

[5] J. M. Tranquada, B. J. Sternlieb, J. D. Axe, Y. Nakamura, and S. Uchida, Nature (London) **375**, 561 (1995).

[6] J. J. Neumeier, G. Wu, A. L. Cornelius, Y. K. Yu, K. Andres, and K. J. McClellan (unpublished).

[7] C. H. Chen, S. W. Cheong, and H. Y. Hwang, J. Appl. Phys. **81**, 4326 (1997).

[8] R. F. Service, Science **283**, 1106 (1999).

[9] V. J. Emery, S. A. Kivelson, and J. M. Tranquada, Proc. Natl. Acad. Sci. U.S.A. **96**, 8814 (1999).

[10] H. Chiba, M. Kikuchi, K. Kusaba, Y. Muraoka, and Y. Syono, Solid State Commun. **99**, 499 (1996).

[11] I. O. Troyanchuk, N. V. Samsonenko, H. Szymezak, and A. Nabialek, J. Solid State Chem. **131**, 144 (1997).

[12] A. Maignan, C. Martin, F. Damay, B. Raveau, and J. Hejtmanek, Phys. Rev. B **58**, 2758 (1998).

[13] A. Maignan, C. Martin, G. V. Tendeloo, M. Hervieu, and B. Raveau, J. Mater. Chem. **8**, 2411 (1998).

[14] J. J. Neumeier and J. L. Cohn, Phys. Rev. B **61**, 14 319 (2000).

[15] M. M. Savosta, P. Novák, M. Marysko, Z. Jirák, J. Hejtmánek, J. Englich, J. Kohout, C. Martin, and B. Raveau, Phys. Rev. B **62**, 9532 (2000).

[16] Y.-R. Chen and P. B. Allen, Phys. Rev. B **64**, 064401 (2001).

[17] E. Granado, C. D. Ling, J. J. Neumeier, J. W. Lynn, and D. N. Argyriou, cond-mat/0303311 (unpublished).

[18] E. Granado, C. D. Ling, J. J. Neumeier, J. W. Lynn, D. N. Argyriou, and P. E. Lee, cond-mat/0303316 (unpublished).

[19] J. A. M. V. Roosmalen and E. H. P. Cordfunke, J. Solid State Chem. **110**, 109 (1994).

[20] J. J. Neumeier (unpublished).

[21] M. R. Lees, O. A. Petrenko, G. Balakrishnan, and D. M. Paul, Phys. Rev. B **59**, 1298 (1999).

[22] B. F. Woodfield, M. L. Wilson, and J. M. Byers, Phys. Rev. Lett. **78**, 3201 (1997).

[23] E. O. Wollan and W. C. Koehler, Phys. Rev. **100**, 545 (1955).

[24] E. Granado, N. O. Moreno, H. Martinho, A. Garcia, J. A. Sanjurjo, I. Torriani, C. Rettori, J. J. Neumeier, and S. B. Oseroff, Phys. Rev. Lett. **86**, 5385 (2001).

[25] J. L. Cohn and J. J. Neumeier, Phys. Rev. B **66**, 100404(R) (2002).

[26] Y. Moritomo, A. Machida, E. Nishibori, M. Takata, and M. Sakata, Phys. Rev. B **64**, 214409 (2001).